







Article

Tackling Microbial Contamination: Safesink Solution with Silver-Coated Microspheres

Eulalia Zumaquero ^{1,*}, David Terrado ¹, Rosa de Llanos ², Marina Puerta ², Rocío Cejudo ²
and María Pilar Gómez-Tena ¹

¹ Instituto de Tecnología Cerámica, Asociación de Investigación de las Industrias Cerámicas, Universitat Jaume I, 12006 Castelló de la Plana, Spain; david.terrado@itc.uji.es (D.T.); pilar.gomez@itc.uji.es (M.P.G.-T.)

² Predepartamental Unit of Medicine, Universitat Jaume I, 12006 Castelló de la Plana, Spain; dellanos@uji.es (R.d.L.); al363040@uji.es (M.P.); rcejudo@fca.uji.es (R.C.)

* Correspondence: eulalia.zumaquero@itc.uji.es; Tel.: +34-964342424

Abstract: Ceramic and vitreous materials can be functionalized to exhibit biocidal activity. This research evaluates the biocidal properties of silver-modified vitreous microspheres designed to be included in water endpoints and siphons to prevent nosocomial diseases produced in hospital environments. The microspheres obtained from a coating and heat treatment process at 650 °C have been chemically and microstructurally characterized using Inductively Coupled Plasma Optical Emission Spectrometry (ICP-OES), Wavelength Dispersive X-ray Fluorescence (WD-XRF), Scanning Electron Microscopy (FEG-SEM) and Energy-dispersive X-ray Microanalysis (EDS) to determine how silver particles are distributed in the glassy matrix and to relate their bactericidal capacity by means of leaching tests. Microbiological tests have been performed against microorganisms such as *Staphylococcus aureus*, *Pseudomonas aeruginosa*, *Escherichia coli*, and *Candida auris*. The results revealed that these silver-coated microspheres had significant bactericidal activity, with a significant reduction in the population of *E. coli*, *C. auris*, and *P. aeruginosa*, with no cytotoxic effect of these microspheres.

Keywords: bacterial; yeast; silver; vitreous; nosocomial disease; biocide activity



Citation: Zumaquero, E.; Terrado, D.; de Llanos, R.; Puerta, M.; Cejudo, R.; Gómez-Tena, M.P. Tackling Microbial Contamination: Safesink Solution with Silver-Coated Microspheres. *Bacteria* **2024**, *3*, 344–357. <https://doi.org/10.3390/bacteria3040023>

Academic Editor: Bart C. Weimer

Received: 11 September 2024

Revised: 7 October 2024

Accepted: 12 October 2024

Published: 16 October 2024



Copyright: © 2024 by the authors. Licensee MDPI, Basel, Switzerland. This article is an open access article distributed under the terms and conditions of the Creative Commons Attribution (CC BY) license (<https://creativecommons.org/licenses/by/4.0/>).

1. Introduction

Nosocomial infections, also known as healthcare-associated infections (HAIs), are a subset of infectious diseases acquired in a healthcare facility that manifest 72 or more hours after the patient's admission to the hospital. These infections can be caused by a wide variety of pathogens, including bacteria, viruses, and fungi.

These infections represent one of the most significant issues in critically ill patients, as they can lead to severe complications such as sepsis and even death. The European EPIC II study unveiled that 44.8% of patients admitted to the intensive care unit (ICU) exhibited some form of infection, with pulmonary infection being the most prevalent (64.7%) [1]. Nosocomial diseases impact millions of patients each year and represent a significant public health issue worldwide. These infections can prolong hospital stays, increase healthcare costs, and diminish patients' quality of life. It is estimated that they can cause up to 100,000 deaths annually in Europe and the United States alone [2–4].

Often, they are caused by multi-drug-resistant pathogens acquired through invasive procedures, excessive or inappropriate use of antibiotics, and non-compliance with infection control and prevention protocols [5].

Methicillin-resistant Staphylococcus aureus (MRSA), *vancomycin-resistant Enterococcus* (VRE), *extended-spectrum β -lactamase* (ESBL)-producing *Enterobacteriaceae*, and multi-drug-resistant *Pseudomonas aeruginosa* [6] and *Acinetobacter baumannii* [7] are the most common bacteria responsible for nosocomial infections. In addition, some of these (MDR) bacteria have become quite prevalent causes of community-acquired infections, which leads to a

large increase in the population at risk and, subsequently, an increase in the number of infections caused by MDR bacteria [8].

Moreover, other pathogens are also involved in nosocomial and community infections; this is the case of *Candida auris*, an emerging MDR fungal pathogen that poses a serious threat to global public health, particularly in healthcare settings. First identified in 2009, *C. auris* has gained attention due to its ability to cause severe nosocomial infections, including bloodstream infections, wound infections, and ear infections, primarily in immunocompromised patients. Unlike other *Candida* species, *C. auris* is notable for its high levels of resistance to commonly used antifungal agents, such as azoles, echinocandins, and, in some cases, amphotericin B. One of the most concerning aspects of *C. auris* is its persistence in hospital environments. It can survive on surfaces for prolonged periods, making it difficult to eradicate and facilitating its spread between patients.

Given their resistance profile, limited treatment options, mortality rates, and the burden on healthcare systems, the World Health Organization (WHO) has published a list of priority pathogens, identifying the most critical bacterial and fungal threats to global public health. This list aims to guide research and development efforts toward new antibiotics, antifungals, alternative treatments, and improved infection control protocols, addressing the growing crisis of antimicrobial resistance [9,10].

The primary measure to prevent infections associated with invasive devices is the removal of the device when it is no longer necessary. Additionally, strict adherence to standard hand hygiene practices and aseptic techniques during the placement and manipulation of invasive devices should be followed [11]. One of the causes that have been associated with the transmission of nosocomial diseases is the generation of aerosols from siphons at water endpoints [12–15]. This article aims to demonstrate, through microbiological analysis, how the addition of silver-coated microspheres to reservoirs such as siphons can provide a solution to the generation of microbial-contaminated aerosols.

Silver has been used as an antimicrobial agent due to its biocidal properties, which can help prevent infections. Its effectiveness against a wide range of microorganisms has been demonstrated, and it has been utilized in various medical and non-medical applications [16–21].

There have been various developments in which different ions have been incorporated into glass to make them biocidal [22–25]. Some of the techniques used to make coatings on ceramic or vitreous materials include immersion, vapor deposition, plasma, sputtering, dip coating, spin coating, spray coating, or roll coating. Each of them offers advantages and disadvantages depending on the material to be coated as well as the specific coating property to acquire [26]. Therefore, a new development of glass microspheres functionalized on their surface was carried out, in which the concentration of silver was enriched on the surface to make it more active and promote controlled leaching of silver ions [27]. This way, the bactericidal effect would prevail over a longer period. The main objective of the development of these functionalized materials is to prevent bacterial growth and the generation of bacteria-carrying aerosols, harnessing the biocidal properties of silver.

In this article, a procedure for evaluating the antimicrobial activity of these microspheres is described, not only in terms of growth inhibition while microbial cells and silver microspheres are in contact [22–25] but also under leaching conditions in aqueous suspensions, as can be the case in siphons. The cytotoxicity of these materials has also been evaluated [28]. The ultimate purpose is to combat nosocomial infections by controlling bacterial growth in water endpoints such as siphons.

2. Materials and Methods

2.1. Preparation of Bioactive Glass Beads

Glass beads acid-washed (G1152 710–1180 μm , Sigma-Aldrich, St. Louis, MO, USA) and colloidal silver (67–75% Ag basis, Sigma-Aldrich) were used to prepare silver-coated glass beads.

The coating process consisted of mixing, by rotation and immersion, the glass beads and an aqueous suspension of colloidal silver with a concentration of silver in the suspension of 0.6%. Simultaneously, the mixture was subjected to a thermal treatment of gradual evaporation of the liquid of the mixture at a temperature of less than 100 °C until obtaining microspheres with a homogeneous silver coating. Subsequently, the microspheres were subjected to a calcination heat treatment in a laboratory furnace at a maximum temperature of 650 °C and in an air atmosphere. The resulting silver glass beads were stirred in distilled water using a magnetic stirrer for 15 min.

2.2. Microstructural Characterization

Original and modified glass beads were analyzed from a chemical and microstructural point of view.

Chemical analysis of glass beads was carried out using the Wavelength Dispersive X-ray Fluorescence method in accordance with the standard procedure using the spectrometer Axios (Panalytical, Almelo, The Netherlands). Samples were dried at 110 °C and prepared by fusion with lithium borate at 1200 °C. The fusion of the samples was conducted in an electric laboratory muffle kiln model IM-1 from ISUNI. The following reference materials were used for calibration in WD-XRF analysis: SRM 91 Opal Glass Powder (NIST), SRM 621 Soda-Lime Container Glass (NIST), SGT G7 Soda-Lime Silica Glass (Society of Glass Technology), SGT G10 Amber Soda-Lime Silica Container Glass (Society of Glass Technology), and AgNO₃ (Merck) [29].

The morphology and chemical composition of glass beads were studied by means of a stereoscopic microscope (OLYMPUS SZX16, Tokyo, Japan), FEG-SEM equipment (QUATROS Thermo Fisher, Waltham, MA, USA), and an energy-dispersive X-ray microanalysis (EDS) instrument (ANAZ-30P-A Thermo Fisher, USA). The SEM-EDS characterization was carried out at 10 kV or 20 kV and high vacuum. This signal provides information on topography and composition. It is more intense the higher the average atomic number of the sample, so that the lighter areas contain heavier elements (compositional contrast) [30]. For the characterization of the beads in the SEM, the beads were first observed and photographed on the surface and then in cross-section, using the backscattered electron signal from a field emission scanning electron microscope. For the SEM cross-section study, the samples were embedded in an epoxy resin and then polished using a diamond abrasive of progressively smaller particle size until the center of the glass beads was reached. Furthermore, the beads were analyzed with EDS equipment connected to the microscope to evaluate the silver content.

2.3. Silver Ion Lixiviation Studies (Release Rate)

The silver cation leaching study was undertaken to determine the short- and long-term durability of the bactericidal coating and to study the wear of the coating in contact with water. For this purpose, several experiments were carried out in discontinuous mode using distilled water and an orbital shaker (SHLD0415DG OHAUS, Parsippany, NJ, USA). A total of 20 g of silver glass beads were weighed in a beaker with 100 mL of distilled water and subjected to mechanical agitation at 400 rpm for a controlled time of 30 min. The distilled water was then removed and replaced with another 100 mL. This operation was repeated until a lixiviation time of 5 h (10 extractions) was reached. The determination of silver in the solutions was carried out by ICP-OES (inductively coupled plasma optical emission spectrometry, model 5100, AGILENT, Santa Clara, CA, USA). The following standard solutions were used to prepare the calibration and validation standards for ICP-OES measurements: commercial standard solutions containing 1000 mg·L⁻¹ of silver (12818, Silver Standard for ICP, MERCK, Barcelona, Spain) and 1 mg·L⁻¹ of silver (69389, Silver Standard for ICP, MERCK).

2.4. Bioactivity Measurement

2.4.1. Microorganisms and Growth Conditions

The antimicrobial activity of silver-coated glass beads was evaluated against different microorganisms: *Staphylococcus aureus* ATCC 29213 and *Pseudomonas aeruginosa* ATCC 27853 (both supplied by the American Type Culture Collection, ATCC, Rockville, MD, USA). *Escherichia coli* CECT 101 (supplied by the Colección Española de Cultivos Tipo, CECT, Valencia, Spain) and *Candida auris* CJ 207 (clinical isolate supplied by La Fe Hospital, Valencia, Spain). Bacterial growth was carried out aerobically overnight at 35 °C in Mueller Hilton Agar plates-MHA (SCHARLAU, Barcelona, Spain). In the case of *C. auris*, yeast growth was performed under the same conditions but in Sabouraud Agar plates-SbA (Scharlau, Spain).

2.4.2. Antibacterial Activity Assays

For this assay, 250 mL sterile flasks containing either 20 g of silver-coated glass beads or no beads (control) were incubated for 60 min at room temperature and shaken at 1500 rpm. During this time, 100 µL aliquots of each condition were taken at different timepoints (0, 10, 20, 30, 45, and 60 min). The aliquots were then subjected to serial dilutions to facilitate plate counting by inoculation of 5 µL drops on the different dilutions. Bacteria were inoculated on MHA plates and incubated at 35 °C for 24 h, except for *Pseudomonas aeruginosa*, whose growth temperature was 30 °C. On the other hand, *Candida auris* was inoculated on SbA plates and incubated at 30 °C for 48 h. After this time, the Colony Forming Units (CFU) were counted, and population reduction was calculated as Log CFU/mL. All experiments were conducted in triplicate to calculate the average and standard deviation.

2.4.3. Antimicrobial Effect of Silver Lixiviation

Following the previous protocol about silver lixiviation, aliquots (named extractions) were taken every 30 min and were used to test their potential antimicrobial activity. Briefly, 8 mL of each extraction was mixed with a microbial suspension of 10⁶ cells/mL. A positive control containing 8 mL of sterile water and the same inoculum was included. Subsequently, the samples were shaken for 3 h at 1500 rpm, and an aliquot was taken every hour. Next, serial dilutions were performed, and drops of 5 µL were inoculated on the different culture media as described above. All experiments were conducted in triplicate to calculate the average and standard deviation.

2.5. Cytotoxicity Investigation

The cytotoxicity study was performed with the silver lixiviation aliquots (extractions) as described above and using the AlamarBlue™ method. Cytotoxicity was found by calculating the percentage of live cells after their exposure to the different extractions [31,32].

To evaluate whether silver lixiviation from silver-coated glass beads was toxic for human use, a cytotoxicity assay was performed with RAW 264.7 cells (*murine monocyte-macrophage cell line*) (*macrophages-like cells*). Cells were first seeded in 96-well plates (10,000 cells/well) in 160 µL of DMEM-10%FBS (DMEM (*Dulbecco's Modified Eagle Medium*) 1× (GIBCO™)); Penicillin/Streptomycin 10,000 U/mL 1% (GIBCO™); HEPES-free acid 1M 1% (Cytiva); L-glutamine, 200 mM 1% (GIBCO™); FBS-qualified (*Fetal Bovine Serum*) 10% (GIBCO™) and were incubated overnight in a 5% CO₂ humidified atmosphere at 37 °C. The next day, 40 µL of each extraction was added to the wells (3 replicates per extraction), and the cells were left for 40 h in the incubator following the same incubation conditions.

After 40 h, the supernatant of the wells was removed, and cells were mixed with 100 µL of a mix of DMEM-2%FBS-AlamarBlue™ Cell Viability Dye (1:10) (Invitrogen, Waltham, MA, USA) in the absence of light. Cells were incubated for 4 h at 37 °C and 5% CO₂, and absorbances were measured at 570 and 600 nm in a Multiscan SkyHigh microplate spectrophotometer (ThermoFisher Scientific, Waltham, MA, USA). Alamar Blue results

were averaged over three independent experiments to calculate the average and standard deviation.

Percentage of cell viability after exposition to the different extractions was calculated by following equation 1 and according to the commercial kit protocol (AlamarBlue™ Cell Viability Dye, (Invitrogen)) [32]:

$$\% = \frac{(O_2 \cdot A_1) - (O_1 \cdot A_2)}{(O_2 \cdot P_1) - (O_1 \cdot P_2)} \cdot 100 \quad (1)$$

where

O_1 = molar extinction coefficient (E) of oxidized alamarBlue (blue) at 570 nm

O_2 = molar extinction coefficient (E) of oxidized alamarBlue at 600 nm

A_1 = absorbance of test wells at 570 nm (mean of 3 replicates)

A_2 = absorbance of test wells at 600 nm (mean of 3 replicates)

P_1 = absorbance of positive growth control well (cells plus alamarBlue but no test agent) at 570 nm (mean of 3 replicates)

P_2 = absorbance of positive growth control well (cells plus alamarBlue but no test agent) at 600 nm (mean of 3 replicates)

3. Results and Discussion

3.1. Microstructural Evaluation of Silver Glass Beads

Both the original glass beads and those obtained after the silver coating process (silver-coated glass beads) were analyzed by X-ray fluorescence to obtain their chemical composition (Table 1). Comparison of the results of the WD-XRF measurements showed that silver-coated glass beads showed 0.69% of silver.

Table 1. Chemical composition of glass beads and silver-coated glass beads by WD-XRF (%).

	SiO ₂	Al ₂ O ₃	B ₂ O ₃	Fe ₂ O ₃	CaO	MgO	Na ₂ O	Ag
Glass Beads	72.3	0.56	<0.15	0.11	8.95	3.85	13.6	<0.01
Ag-Glass Beads	71.9	0.52	<0.15	0.11	8.84	3.80	13.5	0.69

To determine whether the silver present in the glass beads was only on the surface of the bead or if it had been integrated into the glassy matrix, a microstructural study of silver-coated glass beads was carried out using SEM.

For the microstructural characterization of the silver-coated beads, they were analyzed on the surface. The silver-coated glass beads had a shiny coating whose EDS compositional analysis showed the presence of silver. A diffuse whitish-white layer was also observed towards the interior of the bead with the presence of silver. Figure 1 shows one of the beads with the bright white coating as well as the EDS compositional analysis. The whitish and diffuse zones on the surface of the bead and the inside of the bead are also observed. The whitish area (area 1) showed about 1.6% silver, and area 2 showed 0.1% silver in the compositional analysis. The diffuse whitish white layer was analyzed in different locations (A3–A5), observing a high silver content of up to 2.3% silver, decreasing to 0.1% near the center of the bead.

To study the presence and distribution of silver particles in the vitreous matrix, a SEM micrograph was taken at 50,000 magnifications and 10 kV, observing a high amount of silver nanoparticles inside the glassy matrix of approximately 10–20 nanometers (Figure 2).

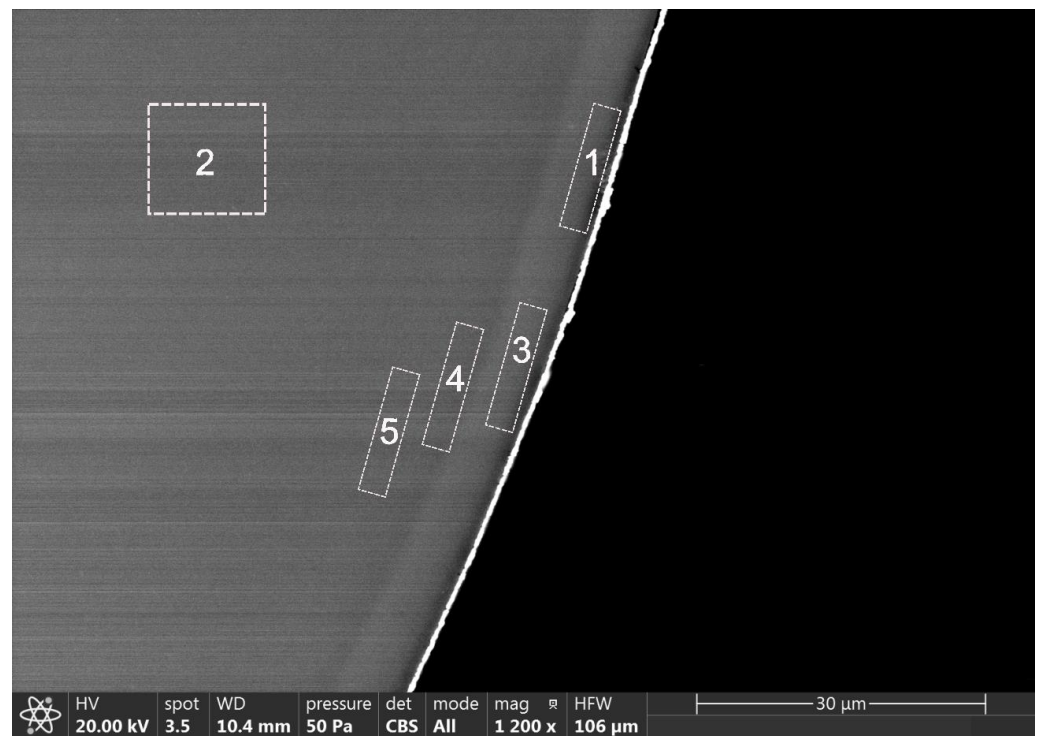


Figure 1. SEM micrograph and EDS analyzed areas of silver-coated glass beads (cross-section).

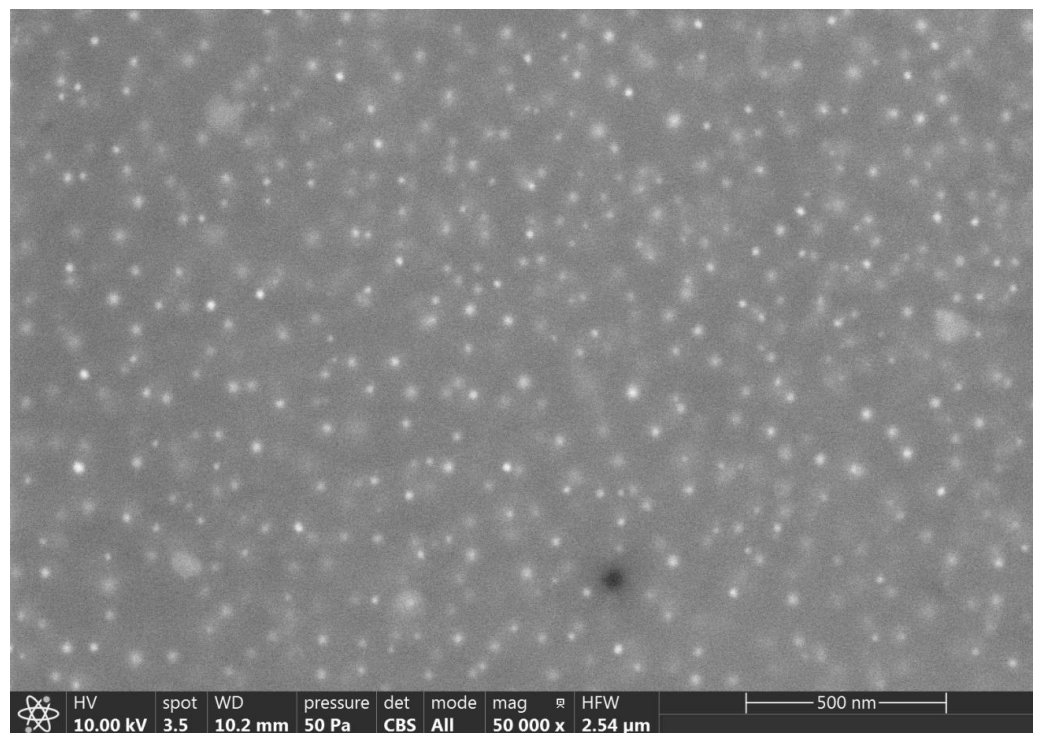


Figure 2. SEM micrograph of silver-coated glass beads (glassy matrix) (50,000×).

For the study of the coating thickness of the silver-coated glass beads, ten beads were chosen, and a micrograph in cross section was taken under the stereo-microscope. Then, the same image was observed in the SEM (Figure 3). Due to the heterogeneity of the coating on the surface of the bead, thickness measurements were performed in four areas of each of the beads (small white points in Figure 3).

The coating thickness measurements made on each of the silver-coated glass beads are shown below in Table 2. The values are expressed as an average value and standard deviation of the four measurements made on each bead. The results obtained from the silver coating thickness study on the selected beads show an average thickness of 3.3 microns.

To try to correlate the color of the bead with the silver content, EDS analysis was also performed in the area corresponding to the white layer of some of the beads (Table 3). It was observed that those beads with a higher percentage of silver in their composition presented a darker golden tone when observed under the stereo-microscope (bead numbers 2 and 3).

Table 2. Coating thickness measurements of the silver-coated glass beads (μm).

Bead Number	Thickness	Bead Number	Thickness
1	3.4 ± 1.8	6	2.2 ± 1.8
2	3.8 ± 1.3	7	4.2 ± 2.1
3	2.4 ± 1.1	8	3.7 ± 0.3
4	3.1 ± 1.3	9	4.4 ± 2.0
5	3.5 ± 1.1	10	1.9 ± 0.2

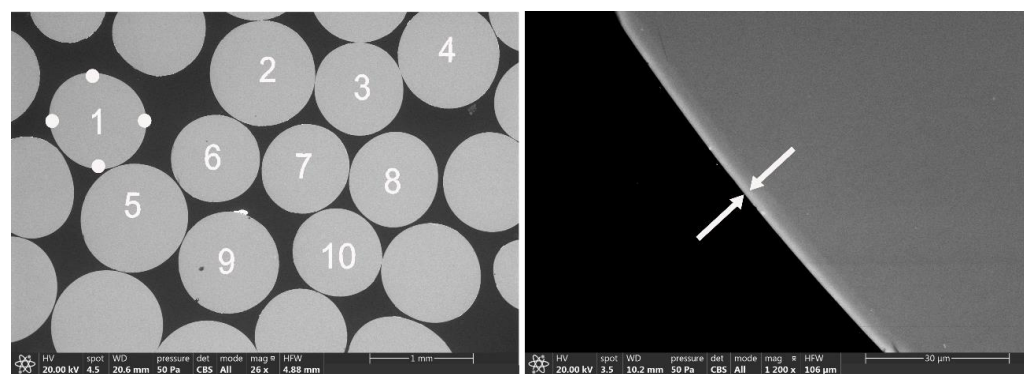


Figure 3. SEM micrograph and coating thickness measurements in cross-section of the silver-coated glass beads. The white arrows indicate the silver coating on the glass bead. The numbers inside the beads are shown in Table 2.

Table 3. Silver content determined by EDS analysis (wt %) on different silver-coated glass beads (cross-section).

Bead Number	Ag (%)	Bead Number	Ag (%)
2	2.09	5	0.77
3	1.50	8	0.83

3.2. Silver Ion Lixiviation Evaluation

This part of the study will focus on the lixiviation of the silver cation to determine the durability of the bactericidal coating in the short term and long term and to evaluate the deterioration or degradation of the coating when it comes into contact with water. For this purpose, several experimental designs will be carried out using distilled water.

To perform these tests, 20 g of silver-coated beads were mechanically agitated in distilled water at 400 rpm. Extractions were performed every 30 min for 5 h (10 extractions). Silver was determined by ICP-OES in the solution obtained. Measurement conditions were optimized to obtain the best signal–noise ratio [33,34]. Once the instrument conditions and analytical line were selected, the construction of the calibration curves was carried out. Once the calibration curves were constructed and validated, samples were analyzed. At least three replicates of each sample were measured to calculate the measurement uncertainty,

which was calculated as $U = k \cdot u_{\text{method}}$, where u_{method} is the combined uncertainty calculated from the uncertainty of the certified value of the reference material, the uncertainty of the measurement of the reference material, and the uncertainty of the measurement of the sample. Coverage factor k was determined from the Student's t -distribution corresponding to the appropriate degrees of freedom and 95% confidence [35,36]. Limit detection and limit quantification for silver in ICP-OES measurements using this methodology were 0.01 and 0.03 $\text{mg} \cdot \text{Kg}^{-1}$, respectively. Table 4 shows the experimental results obtained in the determination of silver using the ICP-OES technique.

Table 4. Results of silver measurement using ICP-OES.

Lixiviation Time (min)	Ag ($\text{mg} \cdot \text{Kg}^{-1}$)	Lixiviation Time	Ag ($\text{mg} \cdot \text{Kg}^{-1}$)
30	9.81 ± 0.02	180	0.23 ± 0.02
60	1.21 ± 0.02	210	0.20 ± 0.02
90	0.52 ± 0.02	240	0.18 ± 0.02
120	0.45 ± 0.02	270	0.21 ± 0.02
150	0.31 ± 0.02	300	0.18 ± 0.02

The results show a high concentration of silver in the suspension 30 min after the beginning of the lixiviation process, possibly due to the silver coating on the surface of the bead. Subsequently, silver cations' lixiviation slows down and stabilizes with values up to 0.18 $\text{mg} \cdot \text{Kg}^{-1}$ at 300 min. This could be explained by the fact that the silver cation would be incorporated in the glassy matrix, and the leaching of the cation into the fluid would occur relatively slowly.

Silver-coated beads were observed under the stereo-microscope after the lixiviation test. The study of beads in both the stereo-microscope and SEM was carried out in cross-section. For this purpose, first a photograph was taken under the stereo-microscope, and then the same image was observed in the SEM (Figure 4). The golden color of the beads after the leaching process showed the presence of silver in the glassy matrix. Therefore, it was decided to carry out an EDS analysis on the surface of the beads at different areas (A1–A4), showing a silver content of up to 1% of silver in the most superficial area (A1), which decreased towards the center of the bead where silver was no longer detected (Figure 5).

The difference found between the original silver-coated bead and the bead observed after the lixiviation process was that in the second one, the silver content on the surface of the bead is lower and decreases quickly towards the center of the bead due to the cation leaching process.

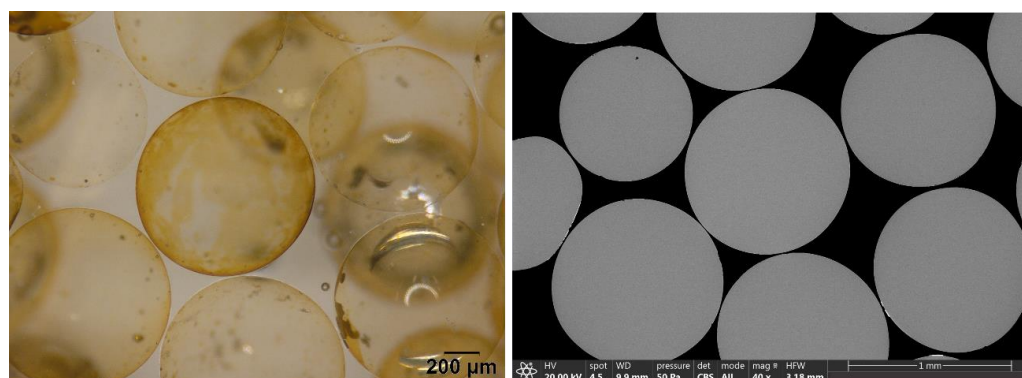


Figure 4. Cross-section of the silver-coated glass beads after the lixiviation process as seen with the stereo-microscope (left) and SEM (right).

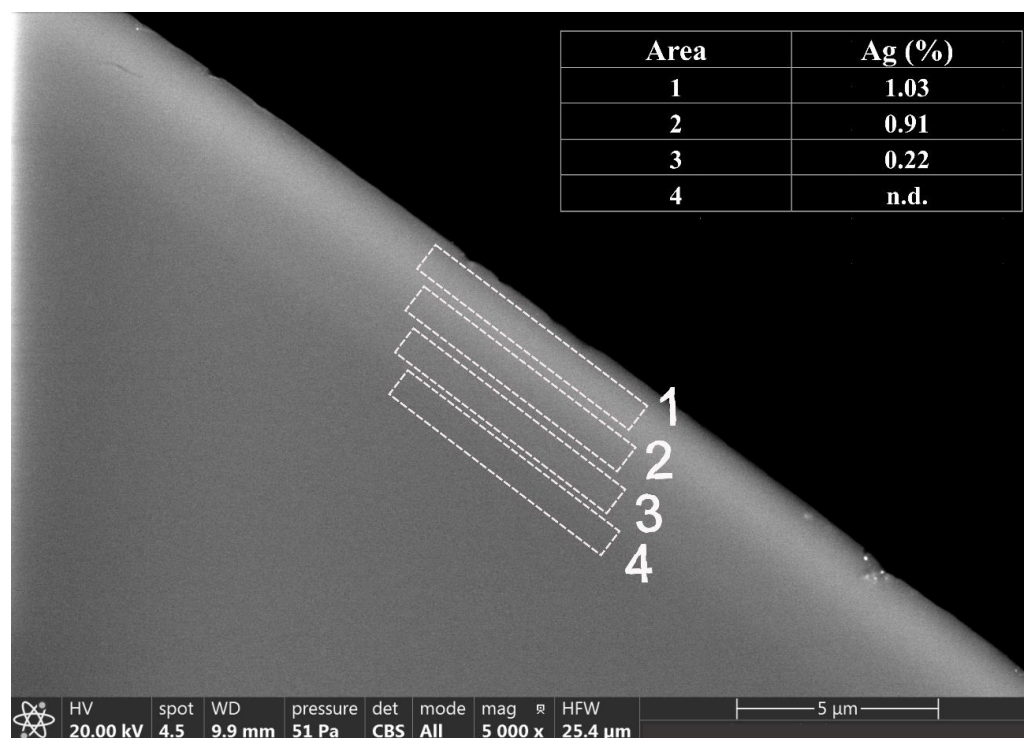


Figure 5. SEM micrograph and EDS analysis (% weight) of the cross-section of silver-coated glass beads after the lixiviation process.

3.3. Bioactivity: Antimicrobial and Cytotoxicity Evaluation of Silver Glass Beads

3.3.1. Antimicrobial Activity

The antimicrobial activity assessment presented in this study provides insights into the effectiveness of silver-coated glass beads against a range of microbial species. The experimental design, which involves exposing known microbial populations to the beads over specified time intervals, offers a systematic and controlled approach to evaluating their bactericidal properties.

Antimicrobial activity was evaluated at different exposure timepoints (0, 10, 20, 30, 45, and 60 min) by quantifying the reduction in the microbial population after exposing a known microbial population to 20 g of silver-coated glass beads contained in a total volume of 100 mL of sterile water (see Section 2). Figure 6 shows the results for the four microbial species tested in this study as the Log₁₀ of CFU/mL for each time and experimental condition.

In the case of *S. aureus* (Figure 6A), a bacterial population reduction was observed over time, being near 3-Logs after 60 min of exposition to silver-coated glass beads. For *E. coli* (Figure 6B), a 3-Log reduction was observed after 10 min of silver exposure and a complete reduction in the population after 20 min. On the other hand, *P. aeruginosa* (Figure 6C) showed similarity to those observed for *E. coli*, and a total population reduction was observed after 20 min of exposure to the silver-coated glass beads. In the case of the yeast species *C. auris*, a reduction in the population was observed over time, and no growth was observed after 30 min with silver-coated glass beads exposure (Figure 6D). In all cases, no reduction was observed in the case of their corresponding positive controls.

The results clearly demonstrate the impact of the silver-coated glass beads on microbial populations. Although the specific antimicrobial mechanisms of these silver-coated glass beads have not been tackled in this study, it seems plausible that silver-coated glass beads might release silver ions, which may be considered microbial killing mechanisms [37].

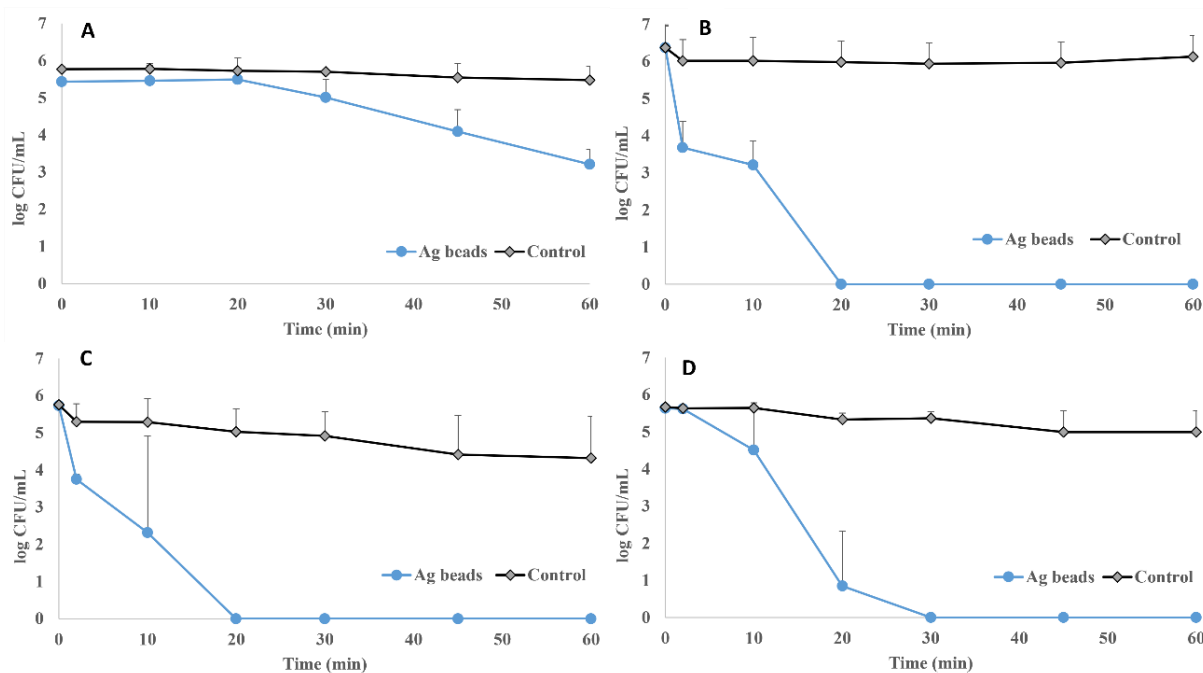


Figure 6. Antimicrobial activity of silver-coated glass beads against a known microbial population of *S. aureus* ATCC 29213 (A), *E. coli* CECT 101 (B), *P. aeruginosa* ATCC 27853 (C), and *C. auris* CJ 207 (D). Experimental condition comparing the effect of silver-coated glass beads and positive control (no beads).

3.3.2. Antimicrobial Activity of Lixiviation Extractions

The antimicrobial activity of the lixiviation extractions was carried out with samples from 30 and 60 min (lixiviation extractions with the highest concentration of silver detected and thus more biocidal activity expected), as well as samples from times 210 and 300 min (those with the lowest amount of silver detected and therefore with less biocidal capacity expected).

These results demonstrate that they play a significant role in microbial killing (Figure 7). Across varying exposure times and concentrations of silver released, high biocidal activity against a range of microbial species was observed. In particular, the 30 min lixiviation extraction sample (with a silver concentration of 9.81 mg L^{-1}) showed a complete bacterial eradication from the beginning in all cases except for *S. aureus*, which was shown after 60 min of exposure, and *E. coli*, in which a partial reduction in the bacterial population was observed (4-log reduction). In the case of a 60 min lixiviation extraction sample (silver concentration of 1.21 mg L^{-1}), similar results were observed. A complete bacterial eradication from time 0 was observed for *P. aeruginosa* and *C. auris*, while in the case of *S. aureus* and *E. coli*, it took 60 min of exposure.

When 210 and 300-min lixiviation extraction samples were used (0.20 and 0.18 mg L^{-1} , respectively), similar results were also observed. Complete bacterial eradication was observed from the beginning in the case of *S. aureus* and *P. aeruginosa*, while for *E. coli* and *C. auris*, it was observed after 60 min of exposure. It is important to highlight that no reduction was observed in the case of the corresponding microbial-positive controls. These results confirm that the antimicrobial activity of silver-coated glass beads can be related to the released silver ions into the medium. The antimicrobial activity of silver ions is well known and can be attributed to several behaviors, such as disturbing the permeability of the cell membrane, binding the sulfur proteins and inactivating them, interrupting the respiratory chain to cause oxidative stress, and interfering with DNA replication to damage the lipids. These phenomena could lead to microbial growth inhibition or even microbial death [37]. These findings underscore the potent bactericidal properties of the silver-coated glass beads, suggesting their potential as a highly effective tool in combating

microbial contamination. The consistency of results across different exposure times and concentrations of silver further bolsters their potential applicability in various settings where microbial control is critical.

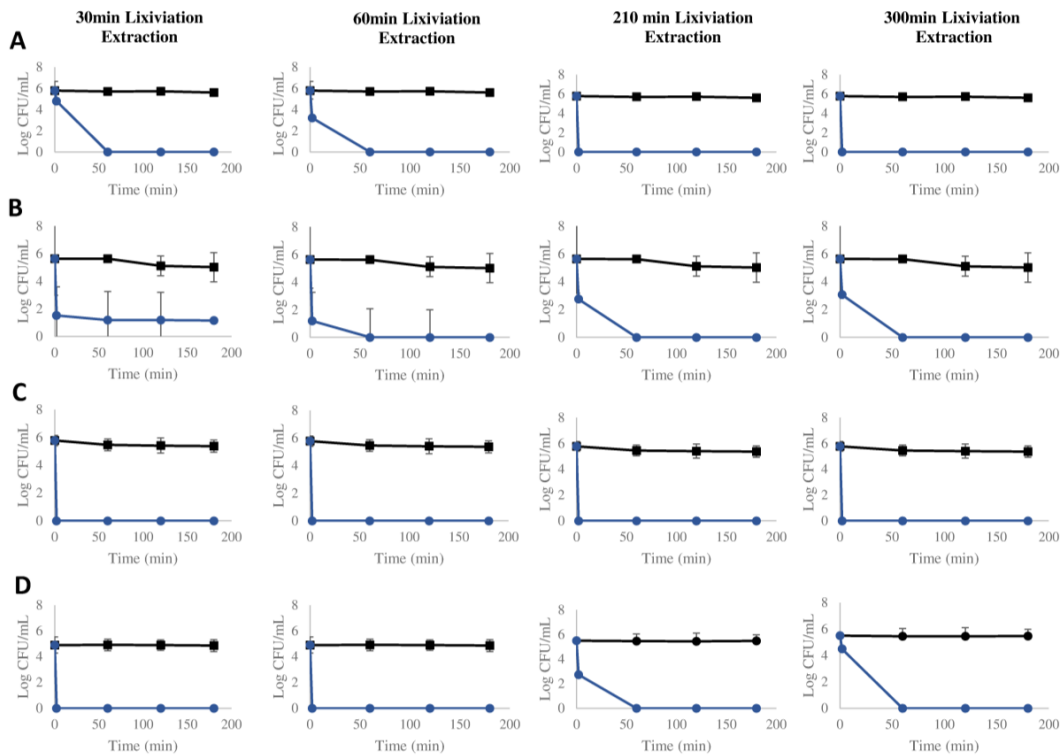


Figure 7. Antimicrobial activity of lixiviation extractions against a known microbial population of *S. aureus* ATCC 29213 (A), *E. coli* CECT 101 (B), *P. aeruginosa* ATCC 27853 (C), and *C. auris* CJ 207 (D). Experimental condition comparing the effect of silver-coated glass beads (blue line) and positive control (no beads) (black line).

3.3.3. Cytotoxicity Evaluation of Lixiviation Extractions

For each extraction, a value of cell viability percentage was obtained and represented in Figure 8. According to the collected data, cell viability was above 95% 48 h post-treatment for all tested extractions. Therefore, no cytotoxic effect was observed from the silver ions released from the silver-coated glass beads.

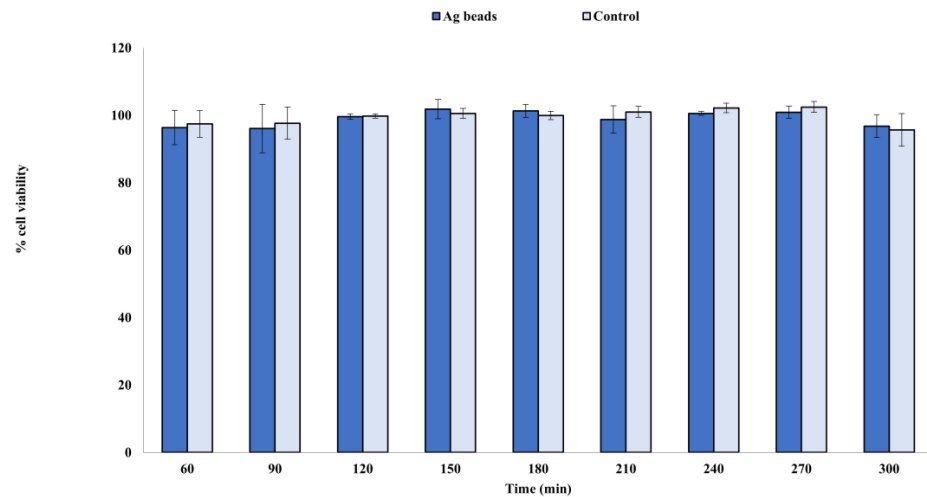


Figure 8. Representation of the average rates of cell viability for the three technical replicates.

4. Conclusions

The silver-coated glass beads were successfully prepared using a controlled coating process with colloidal silver, resulting in a uniform and durable silver coating.

4.1. Microstructural Characterization

Microstructural analysis revealed that the silver content on the surface of the beads was approximately 0.69%, with a coating thickness of the silver-coated glass beads averaged at 3.3 microns, indicating a consistent and effective application process.

4.2. Silver Lixiviation Studies

Silver ion lixiviation studies demonstrated an initial release of silver ions into the solution, which stabilized over time. This suggests that the silver cations were partially incorporated into the glassy matrix, as observed in the SEM.

4.3. Bioactivity

The antimicrobial effect of the lixiviation extractions further confirmed the sustained bactericidal activity of the silver-coated glass beads over time, even with lower concentrations of released silver ions. Antimicrobial testing revealed significant bactericidal activity against *Staphylococcus aureus*, *Escherichia coli*, *Pseudomonas aeruginosa*, and *Candida auris*, with reductions in microbial populations ranging from 3 to 5 Logs after exposure to the silver-coated glass beads.

Moreover, cytotoxicity evaluation showed no significant adverse effects on cell viability, indicating that the silver-coated glass beads did not exhibit cytotoxic properties.

Overall, the silver-coated glass beads demonstrate excellent antimicrobial properties, making them a promising candidate for applications in environments where bacterial contamination poses a threat. Additionally, their non-cytotoxic nature suggests potential for safe use in medical and healthcare settings.

Author Contributions: Conceptualization, M.P.G.-T.; formal analysis, R.d.L.; funding acquisition, M.P.G.-T.; investigation, E.Z., D.T., M.P. and R.C.; methodology, E.Z., R.d.L., R.C. and M.P.G.-T.; project administration, R.d.L. and M.P.G.-T.; resources, R.d.L. and R.C.; visualization, E.Z.; writing—original draft, E.Z.; writing—review and editing, E.Z., R.d.L., R.C. and M.P.G.-T. All authors have read and agreed to the published version of the manuscript.

Funding: This study was funded by Generalitat Valenciana through the Valencian Innovation Agency (Agència Valenciana de la Innovació—AVI) 2021–2023 through project INNVA1/2021/49. RdL was funded by a Beatriz Galindo Fellowship of the Ministerio de Educación y Formación Profesional, Spanish Government (BGP18/00062).

Institutional Review Board Statement: Not applicable.

Informed Consent Statement: Not applicable.

Data Availability Statement: The raw data supporting the conclusions of this article will be made available by the authors on request.

Conflicts of Interest: The authors declare no conflicts of interest.

References

1. Zaragoza, R.; Ramírez, P.; López-Pueyo, M.J. Infección nosocomial en las unidades de cuidados intensivos. *Enferm. Infecc. Microbiol. Clin.* **2014**, *32*, 320–327. [[CrossRef](#)] [[PubMed](#)]
2. White, M.C. Mortality associated with nosocomial infections: Analysis of multiple cause-of-death data. *J. Clin. Epidemiol.* **1993**, *46*, 95–100. [[CrossRef](#)] [[PubMed](#)]
3. Danasekaran, R.; Mani, G.; Annadurai, K. Prevention of healthcare-associated infections: Protecting patients, saving lives. *Int. J. Community Med. Public. Health* **2014**, *1*, 67. [[CrossRef](#)]
4. García-Martín, M.; Lardelli-Claret, P.; Jiménez-Moleón, J.J.; Bueno-Cavanillas, A.; Luna-del-Castillo, J.d.D.; Gálvez-Vargas, R. Proportion of Hospital Deaths Potentially Attributable to Nosocomial Infection. *Infect. Control Hosp. Epidemiol.* **2001**, *22*, 708–714. [[CrossRef](#)] [[PubMed](#)]

5. Types of Healthcare-Associated Infections | HAI | CDC. (n.d.). Available online: <https://www.cdc.gov/HAI/infectionTypes.html> (accessed on 6 June 2023).
6. Jean, S.; Chang, Y.; Lin, W.; Lee, W.; Hsueh, P.; Hsu, C. Epidemiology, treatment, and prevention of nosocomial bacterial pneumonia. *J. Clin. Med.* **2020**, *9*, 275. [[CrossRef](#)]
7. Moubareck, A.; Halat, D. Insights into *Acinetobacter baumannii*: A Review of Microbiological, Virulence, and Resistance Traits in a Threatening Nosocomial Pathogen. *Antibiotics* **2020**, *9*, 119. [[CrossRef](#)] [[PubMed](#)] [[PubMed Central](#)]
8. van Duin, D.; Paterson, D. Multidrug-Resistant Bacteria in the Community: An Update. *Infect. Dis. Clin. N. Am.* **2020**, *34*, 709–722. [[CrossRef](#)] [[PubMed](#)] [[PubMed Central](#)]
9. WHO Bacterial Priority Pathogens List, 2024: Bacterial Pathogens of Public Health Importance to Guide Research, Development and Strategies to Prevent and Control Antimicrobial Resistance. Available online: <https://www.who.int/publications/i/item/9789240093461> (accessed on 4 October 2024).
10. WHO Fungal Priority Pathogens List to Guide Research, Development and Public Health Action. Available online: <https://www.who.int/publications/i/item/9789240060241> (accessed on 4 October 2024).
11. Gould, C.V.; Umscheid, C.A.; Rajender; Agarwal, K.; Kuntz, G.; Pegues, D.A. Guideline for Prevention of Catheter-Associated Urinary Tract Infections (2009). (n.d.). Available online: <https://www.cdc.gov/infectioncontrol/guidelines/cauti/> (accessed on 4 October 2024).
12. Herruzo, R.; Ruiz, G.; Vizcaino, M.J.; Rivas, L.; Pérez-Blanco, V.; Sanchez, M. Microbial competition in environmental nosocomial reservoirs and diffusion capacity of OXA48-Klebsiella pneumoniae: Potential impact on patients and possible control methods. *J. Prev. Med. Hyg.* **2017**, *58*, E34. [[CrossRef](#)]
13. Volling, C.; Ahangari, N.; Bartoszko, J.J.; Coleman, B.L.; Garcia-Jeldes, F.; Jamal, A.J.; Johnstone, J.; Kandel, C.; Kohler, P.; Maltezos, H.C.; et al. Are Sink Drainage Systems a Reservoir for Hospital-Acquired Gammaproteobacteria Colonization and Infection? A Systematic Review. *Open Forum Infect. Dis.* **2020**, *8*. [[CrossRef](#)]
14. De Geyter, D.; Blommaert, L.; Verbraeken, N.; Sevenois, M.; Huyghens, L.; Martini, H.; Covens, L.; Piérard, D.; Wybo, I. The sink as a potential source of transmission of carbapenemase-producing Enterobacteriaceae in the intensive care unit. *Antimicrob. Resist. Infect. Control* **2017**, *6*, 24. [[CrossRef](#)]
15. Sukhum, K.V.; Newcomer, E.P.; Cass, C.; Wallace, M.A.; Johnson, C.; Fine, J.; Sax, S.; Barlet, M.H.; Burnham, C.-A.D.; Dantas, G.; et al. Antibiotic-resistant organisms establish reservoirs in new hospital built environments and are related to patient blood infection isolates. *Commun. Med.* **2022**, *2*, 62. [[CrossRef](#)] [[PubMed](#)]
16. Morones, J.R.; Elechiguerra, J.L.; Camacho, A.; Holt, K.; Kouri, J.B.; Ramírez, J.T.; Yacamán, M.J. The bactericidal effect of silver nanoparticles. *Nanotechnology* **2005**, *16*, 2346–2353. [[CrossRef](#)]
17. Chamakura, K.; Perez-Ballester, R.; Luo, Z.; Bashir, S.; Liu, J. Comparison of bactericidal activities of silver nanoparticles with common chemical disinfectants. *Colloids Surf. B Biointerfaces* **2011**, *84*, 88–96. [[CrossRef](#)]
18. Panáček, A.; Kvítek, L.; Prucek, R.; Kolář, M.; Večeřová, R.; Pizúrová, N.; Sharma, V.K.; Nevěčná, T.; Zbořil, R. Silver colloid nanoparticles: Synthesis, characterization, and their antibacterial activity. *J. Phys. Chem. B* **2006**, *110*, 16248–16253. [[CrossRef](#)] [[PubMed](#)]
19. Kim, J.S.; Kuk, E.; Yu, K.N.; Kim, J.H.; Park, S.J.; Lee, H.J.; Kim, S.H.; Park, Y.K.; Park, Y.H.; Hwang, C.Y.; et al. Antimicrobial effects of silver nanoparticles. *Nanomedicine* **2007**, *3*, 95–101. [[CrossRef](#)]
20. Feng, Q.L.; Wu, J.; Chen, G.Q.; Cui, F.Z.; Kim, T.N.; Kim, J.O. A mechanistic study of the antibacterial effect of silver ions on *Escherichia coli* and *Staphylococcus aureus*. *J. Biomed. Mater. Res.* **2000**, *52*, 662–668. [[CrossRef](#)]
21. Sondi, I.; Salopek-Sondi, B. Silver nanoparticles as antimicrobial agent: A case study on *E. coli* as a model for Gram-negative bacteria. *J. Colloid. Interface Sci.* **2004**, *275*, 177–182. [[CrossRef](#)] [[PubMed](#)]
22. Mubina, M.S.K.; Shailajha, S.; Sankaranarayanan, R.; Saranya, L. In vitro bioactivity, mechanical behavior and antibacterial properties of mesoporous SiO₂-CaO-Na₂O-P₂O₅ nano bioactive glass ceramics. *J. Mech. Behav. Biomed. Mater.* **2019**, *100*, 103379. [[CrossRef](#)]
23. Verné, E.; Ferraris, S.; Miola, M.; Fucale, G.; Maina, G.; Martinasso, G.; Canuto, R.A.; Di Nunzio, S.; Vitale-Brovarone, C. Synthesis and characterisation of bioactive and antibacterial glass-ceramic Part 1—Microstructure, properties and biological behaviour. *Adv. Appl. Ceram.* **2008**, *107*, 234–244. [[CrossRef](#)]
24. Guldiren, D.; Aydın, S. Antimicrobial property of silver, silver-zinc and silver-copper incorporated soda lime glass prepared by ion exchange. *Mater. Sci. Eng. C* **2017**, *78*, 826–832. [[CrossRef](#)]
25. Özgür, C.; Çolak, F.; Şan, O. Preparation, characterization and antimicrobial property of micro-nano sized Na-borosilicate glass powder with spherical shape. *J. Non Cryst. Solids* **2011**, *357*, 116–120. [[CrossRef](#)]
26. Chatzistavrou, X.; Kontonasaki, E.; Paraskevopoulos, K.M.; Koidis, P.; Boccaccini, A.R. 7—Sol-gel derived bioactive glass ceramics for dental applications. In *Non-Metallic Biomaterials for Tooth Repair and Replacement*; Vallittu, P., Ed.; Woodhead Publishing: Sawston, UK, 2013; pp. 194–231. [[CrossRef](#)]
27. Producto Biocida Con Capacidad Bactericida (U 202030264 ES). 2020. Available online: https://bancodepatentes.gva.es/va/turismo-y-calidad-de-vida/-/asset_publisher/xoxK0ZQPXN2u/content/elemento-biocida-esferas-de-vidrio-recubiertas-de-plata-para-el-tratamiento-de-agua (accessed on 3 July 2022).
28. UNE-EN ISO 10993-5; Biological Evaluation of Medical Devices—Part 5: Tests for In Vitro Cytotoxicity. ISO: Geneva, Switzerland, 2009.

29. Gazulla, M.F.; Gómez, M.P.; Orduña, M.; Rodrigo, M. New methodology for sulfur analysis in geological samples by WD-XRF spectrometry. *X-Ray Spectrom.* **2009**, *38*, 3–8. [[CrossRef](#)]
30. Goldstein, J. *Scanning Electron Microscopy and X-ray Microanalysis*, 3rd ed.; Plenum Press: New York, NY, USA, 2003.
31. Ayupova, D.; Dobhal, G.; Laufersky, G.; Nann, T.; Goreham, R.V. An in vitro investigation of cytotoxic effects of InP/ZnS quantum dots with different surface chemistries. *Nanomaterials* **2019**, *9*, 135. [[CrossRef](#)] [[PubMed](#)]
32. Measuring Cytotoxicity or Proliferation—AlamarBlue Assay Protocol | Bio-Rad, Bio-Rad Laboratories Inc. 2023. Available online: <https://www.bio-rad-antibodies.com/measuring-cytotoxicity-proliferation-spectrophotometry-fluorescence-alarBlue.html> (accessed on 13 October 2023).
33. Boss, C.B.; Fredeen, K. *Concepts, Instrumentation and Techniques in Inductively Coupled Plasma Optical Emission Spectrometry*; Perkin Elmer Incorporated: Shelton, CT, USA, 2004.
34. Kaveh, F.; Huang, L.; Beauchemin, D. Inductively Coupled Plasma Optical Emission Spectrometry. *Encycl. Plasma Technol.* **2016**, *1*, 655–678. [[CrossRef](#)]
35. Gazulla, M.F.; Andreu, C.; Rodrigo, M.; Orduña, M.; Ventura, M.J. Development of a rapid and accurate method for the determination of sodium in vacuum gas oils (VGOs) by ICP-OES. *Talanta* **2018**, *188*, 600–605. [[CrossRef](#)]
36. Application Note 1 Comparison of a Measurement Result with the Certified Value. (n.d.). Available online: www.erm-crm.org (accessed on 4 October 2024).
37. Xu, Z.; Zhang, C.; Wang, X.; Liu, D. Release Strategies of Silver Ions from Materials for Bacterial Killing. *ACS Appl. Bio Mater.* **2021**, *4*, 3985–3999. [[CrossRef](#)]

Disclaimer/Publisher’s Note: The statements, opinions and data contained in all publications are solely those of the individual author(s) and contributor(s) and not of MDPI and/or the editor(s). MDPI and/or the editor(s) disclaim responsibility for any injury to people or property resulting from any ideas, methods, instructions or products referred to in the content.